# The Peak Stress Method Applied to Fatigue Strength Assessments of Load Carrying Transverse Fillet Welds with Toe or Root Failures

## G. Meneghetti[1]

**Abstract:** This paper deals with the local approach based on the Notch Stress Intensity Factors (NSIFs) to analyse the fatigue behavior of welded joints. In transverse load carrying fillet-welded joints, failure may occur either at the toe or at the root, depending on the geometry. At the toe, due to the flank angles that are usually encountered in practice, mode I local stresses are singular, while mode II stresses are not. Conversely, at the root of the particular joints analysed in the present paper both mode I and mode II stresses are singular and must be taken into account in fatigue assessments. Recently, a simplified finite element-based method to readily estimate the mode I NSIF and mode II SIF has been proposed (the so-called Peak Stress Method, PSM). According to the PSM, the mode I NSIF and mode II SIF are proportional to the finite values of the opening and sliding stresses, respectively, evaluated at the point of singularity by means of a finite element analysis, as soon as an appropriate mesh pattern is drawn. In this paper the PSM is first summarized and then applied to assess the fatigue strength of load carrying transverse fillet welds, where competition between toe and root failures exists.

**Keywords:** welded joints, local approaches, fatigue, Notch-Stress Intensity Factors, peak stress, finite element method.

## 1 Introduction: Notch Stress Intensity Factors and Peak Stress Method

The Notch-Stress Intensity Factor (NSIF) approach is a well established procedure to assess the fatigue strength of welded joints failing from the weld toe or the weld root. Since the weld toe and root radii $\rho$ cannot be precisely defined and conventional arc-welding technologies lead to small $\rho$ values [Yakubovskii and Valteris (1989), Pang (1993), Seto, Yoshida and Galtier (2004)], the worst case assumption is made, i.e. $\rho$ is set to zero so that NSIFs quantify the intensity of the asymptotic stress distributions in the close neighborhood of the notch tip, as depicted in Fig.

---

[1] Department of Industrial Engineering, University of Padova, via Venezia, 1 – 35131 Padova (Italy)

1. In plane problems, Williams (1952) determined the degree of the singularity of the stress fields due to re-entrant corners, both for mode I and mode II loading. By using a polar coordinate system having the origin at the point of stress singularity, the mode I and mode II NSIFs are [Gross and Mendelson (1972)]:

$$K_1 = \sqrt{2\pi} \cdot \lim_{r \to 0} \left[ \sigma_{\theta\theta, \theta=0} \cdot r^{1-\lambda_1} \right] \tag{1}$$

$$K_2 = \sqrt{2\pi} \cdot \lim_{r \to 0} \left[ \tau_{r\theta, \theta=0} \cdot r^{1-\lambda_2} \right] \tag{2}$$

where $\sigma_{\theta\theta}$ and $\tau_{r\theta}$ are the stress components shown in Fig. 1, $\lambda_1$ and $\lambda_2$ are Williams' first eigenvalues for mode I and mode II, respectively, which depend on the notch opening angle $2\alpha$ and define the stress singularity exponent.
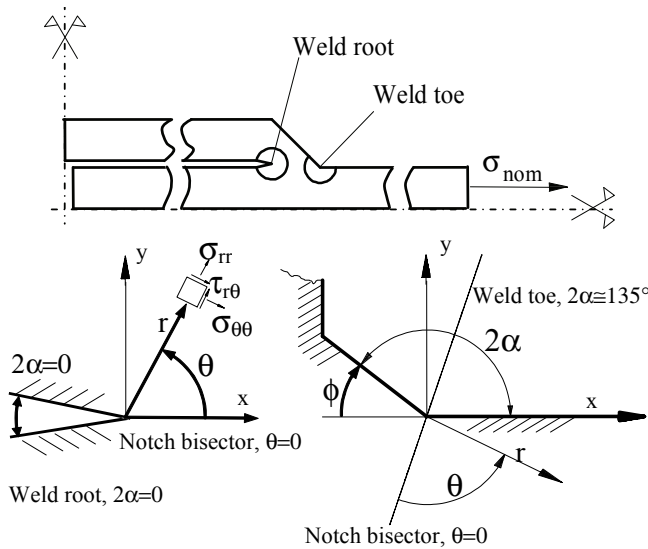


Figure 1: Assumed V-notch geometries at the crack initiation points (the weld toe or the weld root) and description of the local stress components in plane problems; the frame of reference is centred at the point of stress singularity.

Lazzarin and Tovo (1996) determined the following analytical expressions of the local stress distributions close to the V-notch tip as a function of $K_1$ (mode I stresses) and $K_2$ (mode II stresses):

$$\left\{ \begin{array}{c} \sigma_{\theta\theta} \\ \sigma_{rr} \\ \tau_{r\theta} \end{array} \right\} = \frac{1}{\sqrt{2 \cdot \pi}} \cdot \frac{K_1}{r^{(1-\lambda_1)}} \cdot \left\{ \begin{array}{c} f_{1,\theta\theta}(\theta) \\ f_{1,rr}(\theta) \\ f_{1,r\theta}(\theta) \end{array} \right\} + \frac{1}{\sqrt{2 \cdot \pi}} \cdot \frac{K_2}{r^{(1-\lambda_2)}} \cdot \left\{ \begin{array}{c} f_{2,\theta\theta}(\theta) \\ f_{2,rr}(\theta) \\ f_{2,r\theta}(\theta) \end{array} \right\} \tag{3}$$

where the angular functions $f_{ij}$ are known and depend only on the notch opening angle $2\alpha$. Along the notch bisector (see Fig. 1), normal stress components ($\sigma_{\theta\theta,\theta=0}$, $\sigma_{rr,\theta=0}$) are due only to mode I contribution ($f_{2,\theta\theta}(0)=f_{2,rr}(0)=0$), while the shear stress component $\tau_{r\theta,\theta=0}$ is due only to mode II contribution ($f_{1,r\theta}(0)=0$). At the root of welded joints where $2\alpha=0°$ (see Fig. 1), the stress field singularity exponents $\lambda_1$ and $\lambda_2$ are equal to 0.5 according to the Linear Elastic Fracture Mechanics (LEFM). Then Eq. (3) shows that mode I as well as mode II stresses are singular. However, in particular joint geometries, like the so-called TTN analysed later on (see Tab. 3), mode I stresses are by far greater than mode II ones, so that the latter contribution becomes negligible. At the weld toe, the opening angle is typically equal to 135° (see again Fig. 1). Since for $2\alpha > 102°$ the exponent $1-\lambda_2 < 0$, then mode II stresses in Eq. (3) vanish when the distance r tends to zero. In this case, the asymptotic stress distribution is quantified by the mode I NSIF only.

In all cases where only mode I stresses are of interest, the $K_1$ range or the strain range at a fixed distance from the point of singularity were assumed as stress parameters to assess the fatigue life of welded joint [Verreman and Nie (1996), Lazzarin and Tovo (1998), Atzori and Meneghetti (2001)]. It is worth noting that since the scale effect is included in the NSIFs definition, the use of the range of $K_1$, $\Delta K_1$, enabled to rationalize the fatigue test results generated from specimens of very different geometry and absolute dimensions. As a result, two design scatter bands valid for welded joints made of structural steels [Lazzarin and Tovo (1998), Atzori and Meneghetti (2001), Lazzarin and Livieri (2001)] and aluminium alloys [Lazzarin and Livieri (2001)] were proposed, respectively. It is important to highlight that those design fatigue curves were calibrated on test results obtained from specimens. Then, if applied to real (large) components, the estimated fatigue life should be meant as crack initiation life. In fact, in real structures crack propagation paths might be much longer and even multiple with respect to those developed in laboratory specimens: when the propagation of cracks takes place beyond the zone governed by the NSIFs, then the Linear Elastic Fracture Mechanics (LEFM) approach should be used. The NSIF approach has been recently included in a technical book by Radaj, Sonsino and Fricke (2006) dedicated to fatigue analysis of welded joints by local approaches.

The NSIFs can be calculated by means of definitions (1) and (2) applied to the results of linear elastic finite element (FE) analyses. However, very refined mesh patterns are required, which is a drawback when using the local approaches in practical applications. FE sizes on the order of 1 mm or less were adopted by Lazzarin and Tovo (1998), Atzori and Meneghetti (2001) to calculate the NSIFs. The so-called Peak Stress Method (PSM) [Meneghetti (2002), Meneghetti and Lazzarin (2007)] is a FE based approximate procedure to readily estimate the NSIFs parameters by

using rather coarse finite element meshes.

Considering a sharp V-notch subject to pure tensile (mode I) loading, the following expression has been proposed by Meneghetti and Lazzarin (2007):

$$K_{FE}^* = \frac{K_1}{\sigma_{11,peak} \cdot d^{1-\lambda_1}} \cong 1.38 \tag{4}$$

where $K_1$ is the exact NSIF value, $\sigma_{11,peak}$ is the maximum principal stress evaluated by means of a linear elastic finite element analysis at the point of stress singularity and d is mean finite element size adopted to generate the FE mesh. When mode II stresses are different from zero but not of interest, as it usually happens at the toe of welded joints, the maximum principal stress can still be adopted in Eq. (4); conversely, when both mode I and mode II stresses are singular, the opening stress component evaluated along the notch bisector at the point of singularity, $\sigma_{\theta\theta,\theta=0,peak}$, must be adopted in Eq. (4). Fig. 2 shows a typical mesh adopted to analyse a fillet-welded joint with the PSM, where the mean FE size is 1 mm. Fig. 3 shows the peak stresses to use when applying the PSM to assess weld toe or weld root failures, respectively.
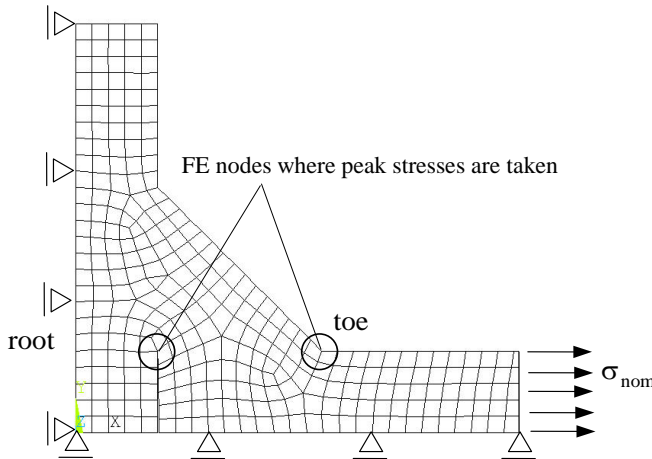


Figure 2: Free mesh used to assess the fatigue strength of a welded joint according to the Peak Stress Method [Meneghetti and Lazzarin (2011)]. The mean element size *d* is the only parameter adopted to generate the free mesh in Ansys code.

In principle the PSM is a simplified FE-based procedure to estimate the NSIF. In fact Eq. (4) establishes a link between the exact NSIF and the linear elastic peak
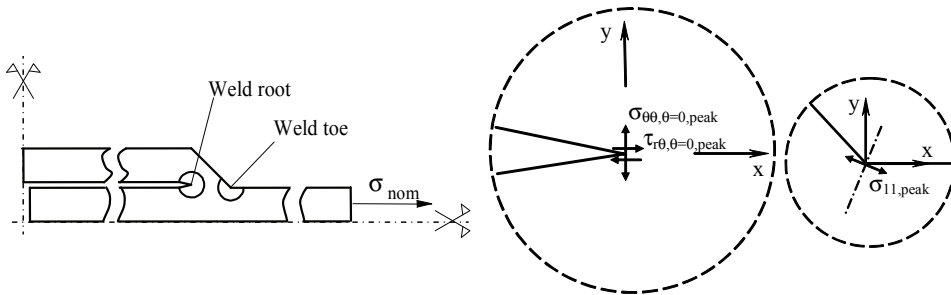
Figure 3: Definition of peak stresses as nodal stresses evaluated by means of a finite element analysis using a mean element size d.

stress evaluated by the FE method. The advantages of the PSM with respect to the direct evaluation of the NSIF by means of definitions (1) and (2) are the following: (i) FE sizes several orders of magnitude greater can be used (Meneghetti and Lazzarin (2007) adopted element sizes around 1 $\mu$m instead of 1 mm or less); (ii) one nodal stress (see Fig. 3) is sufficient to estimate the NSIF rather than processing a set of stress-distance data as required by the application of definitions (1) and (2). The usefulness of the peak stress evaluated by means of a FE analysis was first recognised by Nisitani and Teranishi(2001), Nisitani and Teranishi (2004) concerning the estimation of the mode I SIF at the tip of cracks.

Meneghetti and Lazzarin (2007) derived Eq. (4) under the following conditions:

- use of 4-node linear quadrilateral elements, as implemented in ANSYS numerical code (PLANE 42 of Ansys' element library);

- the pattern of finite elements around the weld toe and the weld root should be that shown in Fig. 2, where only two elements must share the node located at the weld toe whereas four elements share the node located at the weld root; the peak stress is calculated as mean value of the stresses extrapolated at the node of singularity for each element sharing such a node;

- V-notches characterised by an opening angle ranging from 0 to 135 degrees.

It is worth noting that the free mesh generation algorithm available in Ansys has always been used to apply the PSM (see Fig. 2 as an example), the only parameter adopted to drive the algorithm being the so-called 'global element size', which controls the mean element size d. If different element types and different FE codes were used, the coefficient 1.38 of Eq. (4) should be updated. In fact a different

order of the element's shape function and of the extrapolation rules would lead to different peak stresses for the same FE discretization. A comparison between linear and quadratic plane elements was performed by Meneghetti and Valdagno (2002).

Concerning the PSM applied to mode II loading, only the crack case is really of interest, because the root of fillet welded joints can be regarded as a pre-crack from the point of view of the stress analysis. Mode II loading is typical in welded joint geometries like lap joints and cover plates (see Fig. 1), where the weld root is subject to sliding (mode II) stresses, which are prevailing on mode I stresses. To extend the PSM to such stress conditions, a geometry consisting of a crack centred in a plate and subjected to pure mode II loading has been recently considered by Meneghetti and Lazzarin (2011a), as shown in Fig. 4.
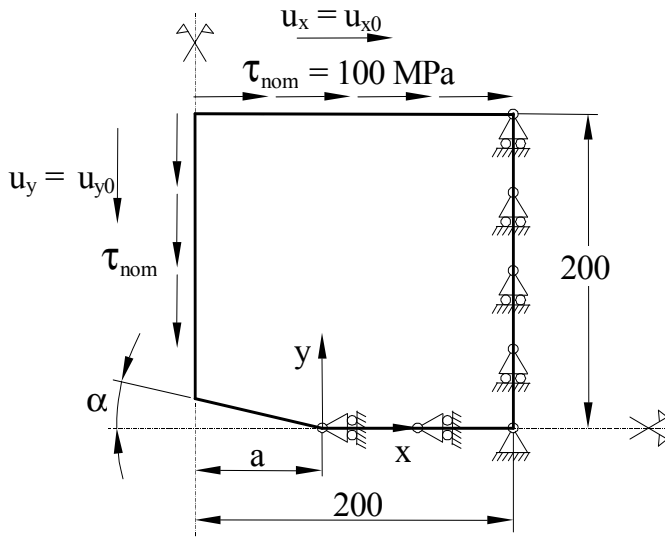


Figure 4: Analysis of a central crack under pure mode II loading. Dimensions in mm [Meneghetti and Lazzarin (2011a)].

Finite element analyses have been performed by using the commercial code Ansys and 4-node quadrilateral elements (PLANE 42 of the Ansys Element Library). For each analysis, the mean element size was fixed between 0.5 mm and 20 mm. Fig. 5 summarisesthe results in terms of the non-dimensional parameter:

$$K_{FE}^{**} = \frac{K_2}{\tau_{xy,peak} \cdot d^{1-\lambda_2}} \tag{5}$$

where $K_2$ is the exact mode II SIF of the considered geometry, $\lambda_2 = 0.5$ and $\tau_{xy,peak}$

is the shear stress component evaluated at the node of stress singularity in the (x,y) coordinate system shown in Fig. 4, where the x-axis is the crack bisector.
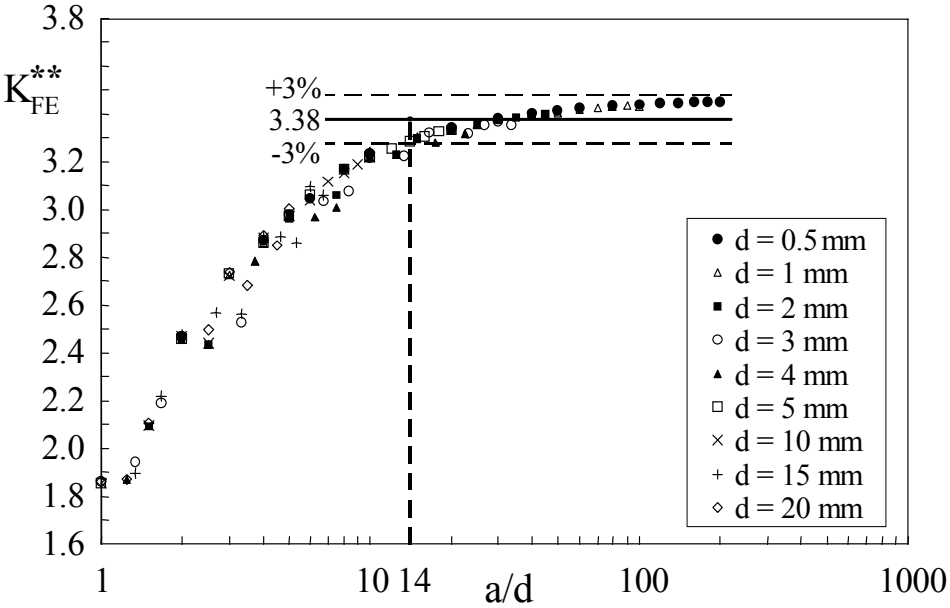


Figure 5: Calibration of the PSM method for a crack ($2\alpha = 0°$) under pure Mode II loading (see Fig. 4); *d* is the mean FE size adopted to generate the free mesh (the 'global element size' command available in Ansys was used).

In Fig.5, $K_{FE}^{**}$ is seen to converge to 3.38 within a scatter band of the numerical results of $\pm 3\%$ for a/d greater than 14. When analyzing the crack problem under pure mode I loading, Meneghetti and Lazzarin (2007) showed that the minimum a/d ratio to assure the validity of Eq. (4) was about 3. Then mode II loading requires smaller FE elements than mode I loading to apply the PSM. In the present paper, convergence of the PSM was checked for each analysed joint geometry by performing an initial FE analysis with a mean element size d equal to 1 mm. Then the FE size was halved in subsequent analyses. The maximum value of d which assured the constancy of the expression ($\tau_{xy,peak} \cdot d^{1-\lambda_2}$) was finally adopted. By means of such a numerical procedure, it was verified that a mean finite element size equal to 1 mm or 0.5 mm could be used. This result is consistent with previous analyses of the author, where a 1-mm-mesh was adopted to apply the PSM to welded joints of complex shape subject to simple mode I loading [Meneghetti (2008), Meneghetti, Atzori and Manara (2010)].

Having in hands Eqs (4) and (5), any fatigue criterion based on the mode I and mode II NSIFs can be re-formulated in an approximate, though simplified, form taking advantage of the PSM. In the next paragraph, a known fatigue strength criterion based on the strain energy density will be considered. Then a proper expression for an equivalent peak stress will be derived in order to assess some weld toe and weld root failures documented in the technical literature.

## 2   Definition of an equivalent peak stress for fatigue strength assessments

To analyse the fatigue strength of welded joints with different flank angles at the weld toe, Lazzarin and Zambardi (2001) proposed to use the range of the total elastic strain energy density (SED) averaged over a sector of radius $R_0$. The use of such parameters enabled the authors to overcome the difficulties associated with the different units of the NSIFs, which depend on the V-notch opening angle according to definitions (1) and (2). Being an elastic stress parameter, the SED range can be expressed as a function of the mode I and mode II NSIFs [Lazzarin and Zambardi (2001)] under plain strain conditions:

$$\Delta \bar{W} = \frac{e_1}{E} \left[ \frac{\Delta K_1}{R_0^{1-\lambda_1}} \right]^2 + \frac{e_2}{E} \left[ \frac{\Delta K_2}{R_0^{1-\lambda_2}} \right]^2 \tag{6}$$

where $e_1$ and $e_2$ depend on the notch opening angle $2\alpha$ and the Poisson's ratio $\nu$. The radius of the structural volume $R_0$ was calibrated on experimental results and turned out 0.28 mm for arc-welded joints in mild steels tested in the as-welded condition under tensile fatigue loading [Lazzarin and Zambardi (2001), Lazzarin, Lassen and Livieri (2003)]. Lazzarin, Berto and Radaj (2009) noted that expression (6) is valid as far as the influence of higher order stress contributions is negligible inside the structural volume. For plate thicknesses on the order of those analysed in the present paper this holds true [Meneghetti and Lazzarin (2011a)]. However, in thin sheet welded joints, such as for example thin lap joints adopted in the automotive industry, validity of Eq. (6) becomes questionable due to the influence of the T-stress, which must be taken into account in the evaluation of the local strain energy density.

By substituting expressions (4) and (5) into Eq (6) and by using the equality $W = (1-\nu^2) \times \sigma_{eq}^2/2E$ valid under plain strain conditions, the equivalent peak stress can be expressed as follows (see Fig.3 for definition of peak stresses):

$$\Delta \sigma_{eq,peak} = \sqrt{f_{w1}^2 \cdot \Delta \sigma_{yy,peak}^2 + f_{w2}^2 \cdot \Delta \tau_{xy,peak}^2} \tag{7}$$

where $f_{w1}$ was given by Meneghetti and Lazzarin (2011):

$$f_{w1} = K_{FE}^* \cdot \sqrt{\frac{2e_1}{1 - v^2}} \cdot \left(\frac{d}{R_0}\right)^{1-\lambda_1} \tag{8}$$

and $f_{w2}$ can be expressed as [Meneghetti and Lazzarin (2011a)]:

$$f_{w2} = K_{FE}^{**} \cdot \sqrt{\frac{2e_2}{1 - v^2}} \cdot \left(\frac{d}{R_0}\right)^{1-\lambda_2} \tag{9}$$

The correction parameters $f_w$ weights the peak stresses both around the V-notch and along the radial direction ($\theta$ direction and r direction in Fig. 1, respectively). According to Equations (8) and (9), it would be convenient to set $d=R_0=0.28$ mm in order to simplify the expressions of $f_{w1}$ and $f_{w2}$. However, according to the assumptions made in previous works [Meneghetti (2008), Meneghetti, Atzori and Manara (2010)], a more coarse mesh has been adopted here and d was set to 1 mm or 0.5 mm.

The peak stresses in Eq. (7), $\Delta\sigma_{yy,peak}$ and $\Delta\tau_{xy,peak}$, are meant to be the opening and sliding stresses at the point of singularity referred to a (x,y) coordinate system where the x-axis coincides with the V-notch (or Alternatively, if we refer to the polar frame of reference shown in Fig. 1, where the direction $\theta=0$ coincides with the V-notch (or crack) bisector, then symbols must be updated, i.e. $\Delta\sigma_{yy,peak}$ is substituted by $\Delta\sigma_{\theta\theta,\theta=0,peak}$ and $\Delta\tau_{xy,peak}$ is replaced by $\Delta\tau_{r\theta,\theta=0,peak}$. The crack bisector (q=0) at the root of the welded geometries considered in the present paper does not coincide always with the x-axis of the (x,y) coordinate system of the FE model. An example of this situation is the TTN geometry which will be analysed later on and is sketched in Fig. 8a. Then, in the present paper the peak stresses will be referred to the polar coordinate system in order to avoid any confusion, as shown in Fig. 3 with reference to the weld root stresses.

The equivalent peak stress (Eq. (7)) can be used to assess weld toe and weld root failures in the presence of mode I and mode II stress distributions. At the weld toe, where mode II stresses are typically non-singular (at least as far as $2\alpha > 102°$), Eq. (7) simplifies to:

$$\Delta\sigma_{eq,peak} = f_{w1} \cdot \Delta\sigma_{11,peak} \tag{10}$$

where $\sigma_{11,peak}$ is the maximum principal stress evaluated at the point of singularity, as shown in the detailed view of the weld toe in Fig. 3. Values of $f_{w1}$ according to Eq. (8) are reported in Tab. 1 for d equal to 0.5 mm and 1 mm, different notch opening angles and $K_{FE}^*=1.38$. Similarly, values of $f_{w2}$ are reported in Tab. 2 for $K_{FE}^{**}=3.38$.

Table 1: Values of parameter $f_{w1}$ according to Eq. (8)

| $2\alpha$ (deg) | $\lambda_1{}^{(a)}$ | $e_1{}^{(a)}$ | $f_{w1,d=0.5mm}{}^{(b)}$ | $f_{w1,d=1mm}{}^{(b)}$ |
|---|---|---|---|---|
| 0 | 0.500 | 0.133 | 0.9970 | 1.410 |
| 90 | 0.544 | 0.145 | 1.015 | 1.392 |
| 110 | 0.586 | 0.136 | 0.9592 | 1.278 |
| 120 | 0.616 | 0.129 | 0.9180 | 1.198 |
| 125 | 0.633 | 0.126 | 0.8984 | 1.159 |
| 135 | 0.674 | 0.118 | 0.8490 | 1.064 |
| 145 | 0.723 | 0.109 | 0.7931 | 0.9610 |
| 150 | 0.752 | 0.104 | 0.7618 | 0.9047 |

[a]: values given by Lazzarin and Zambardi (2001)
[b]: values calculated with $R_0$=0.28 mm, $\nu$=0.3, $K^*_{FE}$=1.38

Table 2: Values of parameter $f_{w2}$ according to Eq. (9)

| 2a (deg) | $\lambda_2{}^{(a)}$ | $e_2{}^{(a)}$ | $f_{w2,d=0.5mm}{}^{(b)}$ | $f_{w2,d=1mm}{}^{(b)}$ |
|---|---|---|---|---|
| 0 | 0.5 | 0.340 | 3.904 | 5.522 |

[a]: values from Lazzarin and Zambardi (2001)
[b]: values calculated with $R_0$=0.28 mm, n=0.3, $K^{**}_{FE}$=3.38

## 3   Definition of a design fatigue curve in terms of equivalent peak stress

Meneghetti and Lazzarin (2011) proposed a design scatter band in terms of equivalent peak stress valid for arc-welded structural steel joints tested in the as-welded conditions. It was calibrated on several published data, mainly due to Maddox (1987), Gurney (1991, 1991a) and Kihl and Sarkani (1997, 1999). Original fatigue strength data were reported in terms of nominal stress applied to the main plate and refer to simple T or cruciform welded joints subjected to axial or bending loadings. For details on welding process, materials, geometries see ref. [Lazzarin and Livieri (2001), Livieri and Lazzarin (2005)]. In summary, all joints were fabricated by arc-welding, the main plate thickness ranged from 6 mm to 100 mm, while the attachment to main plate thickness ratio varied from 0.03 to 8.8. The welded joints were made of structural steels with a yield stress ranging from 360 to 670 MPa. The joints were fatigue tested in the as-welded conditions by applying cyclic loadings with a load ratio R (defined as the ratio between the minimum and the maximum applied load) close to zero. The fatigue cracks nucleated always from the weld toe, where the flank angle $\phi$ was around 45° ($2\alpha$=135°). As a consequence, only the

Mode I stress distributions were singular, so that Eq. (10), instead of Eq. (7), could be used to calculate the equivalent peak stress. In the numerical analyses necessary to convert the original data from the nominal stress applied to the main plate to the equivalent peak stress at the weld toe, a mean element size d equal to 1 mm was adopted. Only for few geometries a mean element size d equal to 0.5 mm had to be adopted to assure convergence of the PSM. Fig. 6 shows the experimental results in terms of equivalent peak stress along with the fatigue curves fitting the experimental data, which were evaluated for 97.7%, 50% and 2.3% survival probabilities. The scatter index $T_\sigma$ resulted equal to 296/156=1.90 when related to mean value $\pm$ two standard deviations and equal to 1.51 when related to 10-90% survival probabilities. The latter value is in agreement with the value 1.50 found for single test series by Haibach (1989).
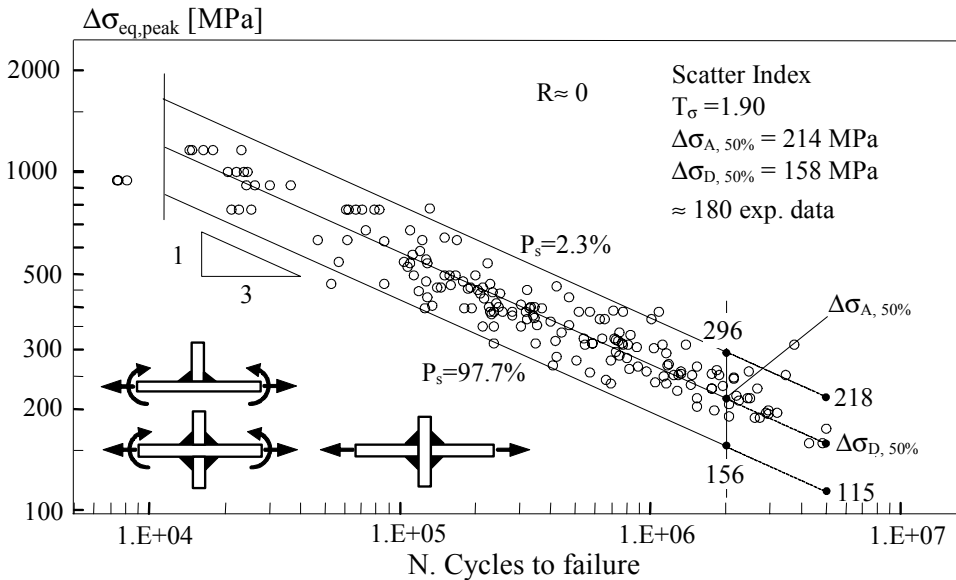


Figure 6: Fatigue strength of steel fillet-welded joints with weld toe failures in terms of equivalent peak stress. The fatigue curves are fitted on the experimental results. The resulting scatter band refer to mean values $\pm$ two standard deviations [Meneghetti and Lazzarin (2011)].

Even if the fatigue curves reported in Fig. 6 were calibrated only on weld toe failures with flank angle around 45°, they are still valid to assess fatigue failures initiated at the weld root in the presence of mode I and mode II stresses as well as at the weld toe in presence of flank angles different from 45° (i.e. $2\alpha \neq 135°$, $2\alpha > 102°$).

Validation of the scatter band reported in Fig. 6 has been recently made by considering about 390 experimental data taken from the literature as well as generated by Meneghetti and Lazzarin (2011a). Fig. 7 reports a comparison between the scatter band reported in previous Fig. 6 and the experimental results analysed by Meneghetti and Lazzarin (2011a), to which the reader is referred for details on specimens geometries, materials and loading conditions. Here we recall that all new data reported in Fig. 7 and not included in previous Fig. 6, refer to transverse fillet-welded joints with toe as well as root failures. The flank angles at the toe $\phi$ ranged between 30° and 70° (150°>$2\alpha$>110°). Concerning root failures, either Eq. (7) or Eq. (10) was applied, depending on the analysed joint geometries. The agreement between the design scatter band and the experimental results shown in Fig. 7 is satisfactory. Some experimental data from weld root failures, which are found to fall below the $P$s=97.7% curve in the low and medium cycle range (from $10^4$ to about $2\times10^5$ cycles), are from the austenitic and the duplex steels.

In the next paragraph the scatter band shown in Fig. 6 will be used to assess the fatigue strength of some load-carrying fillet welded joints, where fatigue failure occurred either at the toe or at the root. In the latter case sliding (mode II) stresses were prevailing on opening (mode I) stresses, so that Eq. (7) had to be used.

## 4   Fatigue test results and evaluation of the peak stresses by means of finite element analyses

A number of fatigue test results published by Macfarlane and Harrison (1965) were considered. The data refer to full load-carrying transverse fillet-welded joints that were tested under pulsating tension fatigue (R=0). The adopted failure criterion was the complete specimens' separation. The materials were two construction steels characterized by a yield stress of 252 and 390 MPa, respectively. The specimens' geometry and the dimensions of the eight test series are reported in Tab. 3. The TTN geometry consists of a cruciform joint, while the CTN and HCTN geometries are lap joints. While the test results of the TTN1 and TTN2 series had already been considered previously by Meneghetti and Lazzarin (2011), the remaining six test series reported in Tab. 3 have never been analysed previously by the present author. Due to the particular geometries, both toe failures (where only mode I stresses are of interest) and root failures (where mode II stresses are prevailing) were documented in the original paper. Then these tests are critical to validate the use of the equivalent peak stress.

Two-dimensional finite element analyses of the joint geometries were performed by means of Ansys rel. 12 code. One-fourth of the geometry was modeled, taking advantage of the symmetry conditions. Four-node quadrilateral elements (PLANE 42 elements of the Ansys element library) were adopted to generate the free mesh
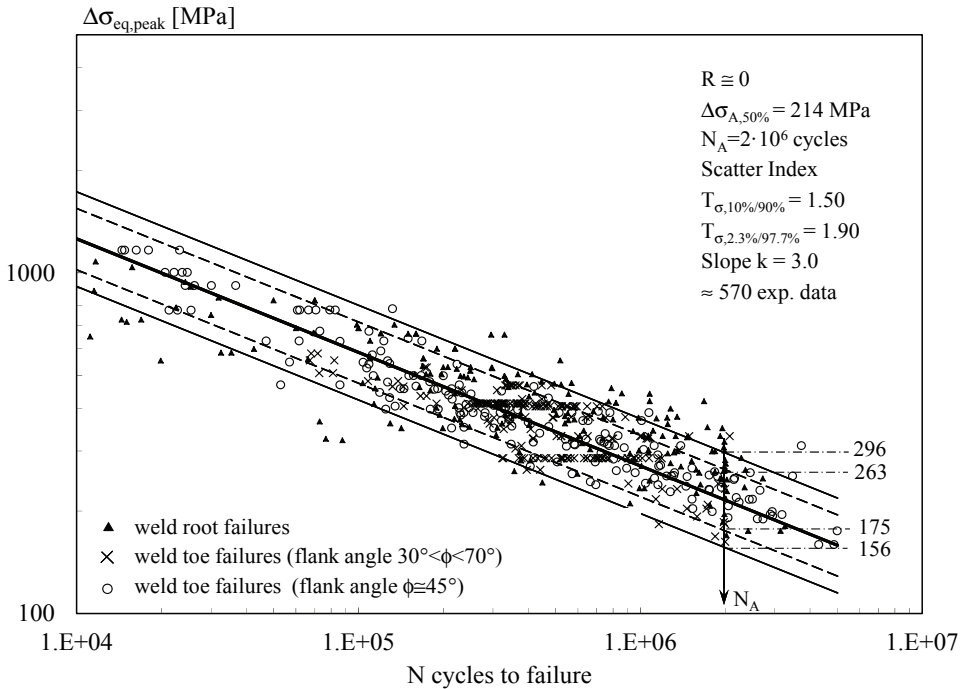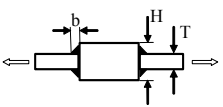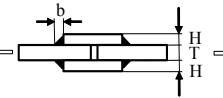
Figure 7: Comparison between the scatter band reported in Fig. 6 and the fatigue strength of steel welded joints with weld toe or weld root failures in terms of the equivalent peak stress. Scatter bands have been calibrated only on weld toe failures with flank angle $\phi$=45˚ ("o" symbols) and are related to mean values $\pm$ two standard deviations ($T_\sigma$=296/156=1.90) or to $P_s$=10-90% ($T_\sigma$=263/175=1.50). For original data see [Meneghetti and Lazzarin (2011a)].

characterized by a mean element size *d*. In order to input the parameter *d*, the '*global element size*' command available in the pre-processor environment of the software was adopted. No additional tools were used to drive the free mesh generation algorithm. Fig.8 reports as an example the FE mesh adopted for a CTN- and a TTN-type geometry, respectively, where d was set to 1 mm. Surface-to-surface, friction-free contact elements were generated between the main and the cover plates of the CTN geometries.

While convergence of the peak stress method at the toe of all joint geometries could have been achieved by setting d=1mm, strictly speaking that was not true at the root of CTN geometries, where mode II stresses are prevailing. In fact it has been underlined that the PSM is more critical to converge in case of mode II than mode I loading. As aforementioned, to analyse convergence of the PSM at the root of CTN

Table 3: Joint geometries and materials analysed by Macfarlane and Harrison (1965). The length of the central block (TTN geometry) and of the cover plate (CTN geometry) is 114 mm.

| Joint geometry | Test series | Steel Material | Yield Stress [MPa] | T [mm] | H [mm] | b [mm] |
|---|---|---|---|---|---|---|
|  | TTN1 | BS 15 | 252 | 12.7 | 31.75 | 7.94 |
| | TTN2 | | | 12.7 | 38.1 | 12.7 |
| | TTN3 | | | 7.94 | 38.1 | 12.7 |
|  | HCTN 1 | BS 968 | 390 | 7.94 | 7.94 | 7.94 |
| | CTN 2 | BS 15 | 252 | 12.7 | 7.94 | 7.94 |
| | CTN 3 | | | 12.7 | 12.7 | 7.94 |
| | CTN 4 | | | 12.7 | 12.7 | 12.7 |
| | HCTN 5 | BS 968 | 390 | 19.05 | 19.05 | 19.05 |

joints the following procedure was adopted: the quantity $[\tau_{\theta\theta,\theta=0,peak}\cdot d^{(1-1/2)}]$ was first calculated by using a mean FE size d equal to 1 mm and then it was re-evaluated in subsequent analyses by progressively halving the mean element size $d$ at each step until constancy of the result between the present and the previous FE solution was obtained. As a result, a mean element size $d$=0.5 mm had to be adopted for HCTN1, HCTN5, CTN2 and CTN 4 geometries, while an increased size $d$=1 mm could be used for the remaining geometries.

Tab. 4 summarises the relevant peak stresses evaluated at the potential crack initiation sites (the toe and the root of welds) along with the equivalent peak stresses calculated with a reference nominal stress equal to 100 MPa. In order to apply the peak stress method, eq. (7) was adopted at the root of CTN geometries, where both mode I and mode II stresses exist. In particular Tab. 4 shows that compressive stresses $\Delta\sigma_{\theta\theta,\theta=0,peak}$ are calculated there.However, the equivalent peak stress Eq. (7) does not distinguish the sign of stresses. Concerning the treatment of negative peak stresses, first of all we note that referring to the particular geometries under analysis, the contribution of the mode I stress on the equivalent peak stress at the root of CTN joints is negligible. In fact take for example the HCTN 5 geometry, where the ratio between the opening and the sliding peak stresses at the root is the highest and equal to 24.58/70.17=0.35. If the equivalent peak stress had been calculated by using only the sliding peak stress, a value of 274.0 MPa would have
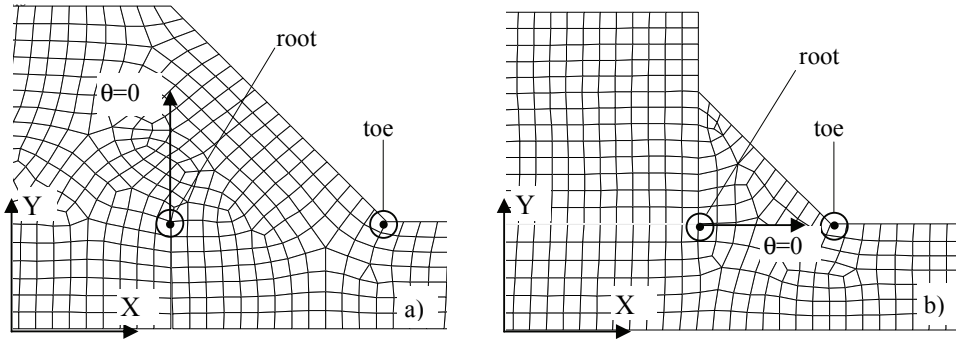
Figure 8: Examples of FE mesh generated in Ansys code (free mesh, mean element size d=1 mm, four-node quadrilateral elements PLANE 42) for TTN (a) and CTN (b) geometries. For the CTN geometry friction-free contact elements have been used between main and cover plates. The geometries analysed by using a mean element size equal to 0.5 mm are highlighted in Tab. 4.

been obtained. Such a stress is practically coincident with 275.1 MPa, which has been calculated by means of Eq. (7) and is reported in Tab. 4. In a more general case, if compressive stresses were prevailing, the accuracy of fatigue strength estimations performed by using the equivalent peak stress combined with the scatter band shown in Fig. 6 would certainly decrease, even if on the safe side, as shown by Lazzarin et al. (2009a). This is simply because that scatter band was calibrated on experimental results where fatigue cracks (at the weld toe) were subjected to tensile (opening) rather than compressive stresses.

Concerning the TTN geometries, stresses at the root flow along a direction approximately normal to the crack bisector (the direction $\theta=0$ in Fig. 8a), so that the opening peak stress $\Delta\sigma_{\theta\theta}$ is well higher than the shear stress $\Delta\tau_{r\theta}$, as reported in Tab.4. That is why in a previous paper, where only the TTN1 and TTN2 geometries had been considered, Meneghetti and Lazzarin (2011) calculated the peak stress at the root by using Eq. (10). In the present paper Eq. (7) was applied rigorously. However, the maximum difference between the equivalent peak stress evaluated by means of the two approaches is limited to 10% in the worst case represented by the TTN1 geometry. Finally, at the toe of all considered geometries Eq. (10) was always applied, because mode II stresses are non-singular.

Table 4: Stress parameters calculated at the toe and at the root of the joints tested in the present work. The nominal stress applied to the main plate is $\Delta\sigma_{nom} = 100$ MPa. Peak stresses evaluated by means of a free mesh, mean finite element size d equal to 1 mm or 0.5 mm and four-node quadrilateral elements (PLANE 42 of the Ansys Element library).

| Series | $\Delta\sigma_{\theta\theta,\theta=0,peak}$ [MPa] | $\Delta\tau_{r\theta,\theta=0,peak}$ [MPa] | $\Delta\sigma_{11,peak}$ [MPa] | $\Delta\sigma_{eq,peak}$ [MPa] | | Failure position |
|---|---|---|---|---|---|---|
| | Root | Root | Toe | Root[o] | Toe[oo] | |
| TTN1 | 286.2 | 42.00 | 305.7 | 415.8 | 325.3 | Root (8) |
| TTN2 | 207.8 | 20.18 | 232.0 | 313.5 | 246.9 | Root (7) |
| TTN3 | 104.9 | 13.70 | 176.0 | 166.1 | 187.3 | Toe (6), Run-out (2) |
| HCTN 1 | -15.03** | 50.20** | 230.4** | 196.6 | 195.6 | Toe (7), Root (1) |
| CTN 2 | -19.00** | 88.10** | 332.6** | 344.5 | 282.4 | Root (7), Toe (1) |
| CTN 3 | -3.22 | 62.83 | 265.1 | 347.0 | 282.1 | Toe (5), Root (3) |
| CTN 4 | -14.44** | 64.86** | 278.7** | 253.6 | 236.6 | Toe (6), Root (1) |
| HCTN 5 | -24.58** | 70.17** | 318.2** | 275.1 | 270.1 | Toe (6), Root (1) |

[o]: calculated by means of Eq. (7)
[oo]: calculated by means of Eq. (10)
**: calculated with d=0.5 mm

## 5   Assessments of toe and root failures by means of the Peak Stress Method

Tab. 4 reports also the failures locations which were documented by Macfarlane and Harrison (1965) in the original paper. It is seen that in most cases the peak stress correctly predicts the failure location, since it is higher where crack initiation takes place (TTN1, TTN2, TTN3, CTN2 geometries). Similar values of the equivalent peak stress were calculated at the root and at the toe in the case of HCTN1 and HCTN5 specimens, where at least one failure starting from each position was observed experimentally. In the case of CTN4 geometry, the experimental failure position was the toe for six among the seven tested specimens, while the equivalent peak stress is higher at the root. However it should be noted that the difference between peak stresses evaluated at the toe and at the root is only 7%. In the case of CTN3 specimens, the equivalent peak stress is 23% higher at the root than at the toe. However five among the eight tested specimens failed at the toe.

Fig. 9 reports the experimental results in terms of equivalent peak stress evaluated at the point of crack initiation (either the toe or the root) observed experimentally. In the same figure the scatter band previously shown in Fig. 6 and 7 is reported for comparison. It is seen that the agreement between the design scatter band and the
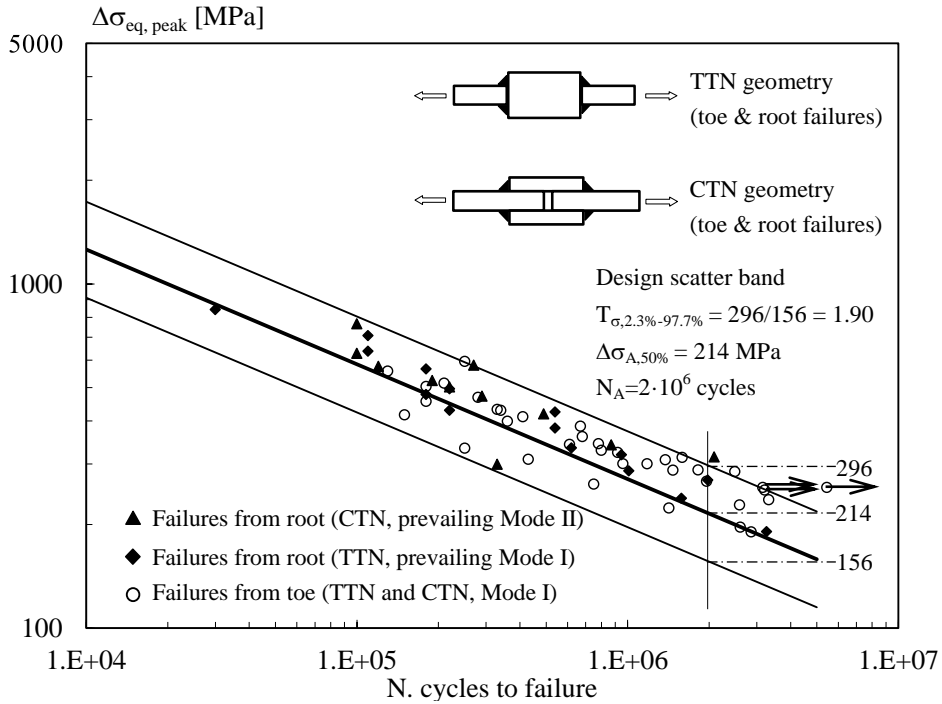
experimental results is satisfactory.



Figure 9: Comparison between fatigue test results and design scatter band reported in Fig. 6 in terms of equivalent peak stress evaluated by means of FE analyses (see Eqs. (7) and (10)) at the weld toe or root.

## 6  Conclusions

The peak stress method is a simplified, finite-element-based technique to readily estimate the Notch Stress Intensity Factors (NSIFs). In principle, any fatigue model that involves the NSIFs can be re-formulated in a simplified form by using the peak stresses evaluated at the points of stress singularity. In the present paper a link between the peak stresses and the strain energy density averaged in a structural volume has been shown. As a result, an equivalent peak stress could be defined, which combines the opening and the sliding stresses evaluated at the point of singularity by means of a finite element analysis with a fixed mean element size. The equivalent peak stress is a design stress that in the present paper has been used in combination with a previously defined scatter band to assess weld toe and weld root

fatigue failures of full load-carrying transverse fillet-welded joints. According to the experimental data considered here, the peak stress correctly discriminates weld root from weld toe failures. In few cases, when the difference between the equivalent peak stress evaluated at the toe and at the root is limited to about 20% or less, a reduced correlation between anticipated and experimental crack initiation locations has been found. In subsequent analyses the equivalent peak stress evaluated at the experimental crack initiation point has been used for fatigue strength estimations. By summarizing all available data, a good agreement between theoretical and experimental fatigue lives has been found.

## References

**Atzori, B.; Meneghetti, G.** (2001): Fatigue strength of fillet welded structural steels: finite elements, strain gauges and reality. *Int. J. Fatigue*, vol. 23, pp. 713-721.

**Gross, R.; Mendelson, A.** (1972): Plane Elastostatic Analysis of V-Notched Plates. *Int. J. Fract. Mech.*, vol. 8, pp. 267-272.

**Gurney, T. R.** (1991): *The fatigue strength of transverse fillet welded joints*. Abington Publishing, Abington, Cambridge.

**Gurney, T. R.** (1991a): *Fatigue of thin walled joints under complex loading*. Abington Publishing, Abington, Cambridge.

**Haibach, E.** (1989): Service fatigue-strength-methods and data for structural analysis, VDI, Dusseldorf.

**Kihl, D.P.; Sarkani, S.** (1997): Thickness effects on the fatigue strength of welded steel cruciforms. *Int. J. Fatigue*, vol. 19, S311-S316.

**Kihl, D.P.; Sarkani, S.** (1999): Mean stress effects in fatigue of welded steel joints. *Probabilist. Eng. Mech.*, vol. 14, pp. 97-104.

**Lazzarin, P.; Tovo, R.** (1996): A unified approach to the evaluation of linear elastic fields in the neighborhood of cracks and notches. *Int. J. Fract.*, vol. 78, pp. 3-19.

**Lazzarin, P.; Tovo, R.** (1998): A notch intensity factor approach to the stress analysis of welds. *Fatigue Fract. Engng Mater. Struct.*, vol. 21, pp. 1089-1103.

**Lazzarin, P.; Livieri, P.** (2001): Notch stress intensity factors and fatigue strength of aluminium and steel welded joints. *Int. J. Fatigue*, vol.23, pp. 225-232.

**Lazzarin, P.; Zambardi, R.** (2001): A finite-volume-energy based approach to predict the static and fatigue behaviour of components with sharp V-shaped notches. *Int. J. Fracture*, vol. 112, pp. 275-298.

**Lazzarin, P.; Lassen, T.; Livieri, P.** (2003): A Notch Stress Intensity approach applied to fatigue life predictions of welded joints with different local toe geometry.

*Fatigue Fract. Engng Mater. Struct.*, vol. 26, pp. 49-58.

**Lazzarin, P.; Berto, F.; Radaj, D.** (2009): Fatigue-relevant stress field parameters of welded lap joints: pointed slit tip versus keyhole notch. *Fatigue Fract. Engng Mater. Struct.*, vol. 32, pp. 713-735.

**Lazzarin, P.; Meneghetti, G.; Berto, F.; Zappalorto, M.** (2009a): Practical application of the N-SIF approach in fatigue strength assessment of welded joints. *Welding in the World*, vol. 53, no. 3/4, pp. R76-R89.

**Livieri, P.; Lazzarin, P.** (2005): Fatigue strength of steel and aluminium welded joints based on generalised stress intensity factors and local strain energy values. *Int. J. Fracture*, vol. 133, pp. 247-278.

**Yakubovskii, V.V.;Valteris, I.J.**(1989): Geometrical parameters of butt and fillet welds and their influence on the welded joint fatigue life. *IIW Document XIII 1326–89*.

**Macfarlane, D. S.; Harrison, J. D.** (1965): Some fatigue tests of load carrying transverse fillet welds. *British Welding Journal*, vol. 12, no. 12, pp.613-623.

**Maddox, S. J.** (1987): *The effect of plate thickness on the fatigue strength of fillet welded joints.* Abington Publishing, Abington, Cambridge.

**Meneghetti G.** (2002): Simplified evaluation of the local stresses in welded joints. *Rivista italiana della saldatura*, no. 4, pp. 499-505 (in italian).

**Meneghetti G.; Valdagno L.** (2002): *The use of peak stresses evaluated by FEM in crack-like notches subjected to fatigue loadings.* Proceedings of the 31$^{st}$ AIAS National Conference (in italian).

**Meneghetti, G.; Lazzarin, P.** (2007): Significance of the Elastic Peak Stress evaluated by FE analyses at the point of singularity of sharp V-notched components. *Fatigue Fract. Engng Mater. Struct.*, vol. 30, pp. 95-106.

**Meneghetti, G.** (2008): The peak stress method applied to fatigue assessments of steel and aluminium fillet welded joints subjected to mode-I loading. *Fatigue Fract. Engng Mater. Struct.*, vol. 31, pp. 346–369.

**Meneghetti, G.; Atzori, B.; Manara, G.** (2010): The Peak Stress Method applied to fatigue assessments of steel tubular welded joints subject to Mode-I loading. *Eng. Fract. Mech.*, vol. 77, pp. 2100-2114.

**Meneghetti, G.; Lazzarin, P.** (2011): The peak stress method for fatigue strength assessments of welded joints with weld toe or weld root failures. *Welding in the World*, vol. 55(7/8), pp. 22-29.

**Meneghetti, G.; Lazzarin, P.** (2011a): The use of peak stresses for fatigue strength assessments of welded lap joints and coverplates with toe and root failures. *IIW doc. XIII-2375-11*.

**Nisitani, H.; Teranishi, T.** (2001): *$K_I$ value of a circumferential crack emanating from an ellipsoidal cavity obtained by the crack tip stress method in FEM*. In: Guagliano M, Aliabadi MH, editors. Proceedings of the 2$^{nd}$ International Conference on Fracture and Damage Mechanics FDM, pp. 141–146.

**Nisitani, H.; Teranishi, T.** (2004): $K_I$ value of a circumferential crack emanating from an ellipsoidal cavity obtained by the crack tip stress method in FEM. *Eng. Fract. Mech.*, vol. 71, pp. 579–585.

**Pang, H.J.L.** (1993): Analysis of weld toe profiles and weld toe cracks. *Int. J. Fatigue*,vol. 15, pp. 31–36.

**Radaj, D.; Sonsino, C.M.; Fricke, W.** (2006): *Fatigue assessment of welded joints by local approaches*. 2$^{nd}$ ed. Cambridge/Boca Raton Fla: Woodhead Publishing/CRC Press.

**Seto, A.; Yoshida, Y.;Galtier, A.** (2004): Fatigue properties of arc-welded lap joints with weld start and end points. *Fatigue Fract. Engng Mater. Struct.,* vol. 27, pp. 1147–1155.

**Verreman, Y.; Nie, B.** (1996): Early development of fatigue cracking at manual fillet welds. *Fatigue Fract. Engng Mater. Struct.*, vol. 19, pp. 669–681.

**Williams, M.L.** (1952): Stress singularities resulting from various boundary conditions in angular corners on plates in tension. *J. Appl. Mech.,*vol. 19, pp. 526-528.